Materials Today: Proceedings xxx (xxxx) 1–4

Contents lists available at ScienceDirect

Materials Today: Proceedings

journal homepage: www.elsevier.com

Journal Cover Image

Synthesis and thermal stability of ferrites added polymers nanocomposites

P. Raju [a, *], A Thirupathi [b], Ch. Kalyani [a], Sk. Mahammed Ali [a], J. Shankar [a], G. Neeraja Rani [a], J. Anjaiah [a], M. Kanaka Durga [a]

[a] Geethanjali College of Engineering and Technology, Cheeryal, Hyderabad 501301, India
[b] Malla Reddy Engineering College, Gundlapochampally, Telangana 500100, India

ARTICLE INFO

Keywords:
Nanocomposites
Ferrite
Polymer
Thermogravimetric analysis
Mechanical alloying

ABSTRACT

Nanocomposites of ferrite and polymer constituents with the ordered combination (x) wt% $Ni_{0.48}Cu_{0.12}Zn_{0.4}Fe_2O_4$ + (1-x) wt% polyaniline, ($0 \le x \le 1$) and (x) wt% (NCZ-PANI), $Ni_{0.48}Cu_{0.12}Zn_{0.4}Fe_2O_4$ + (1-x) wt% paraformaldehyde, ($0 \le x \le 1$) (NCZ-PFD) were prepared by mechanical alloying method. A microwave digestion system was used to prepare nanopowders of $Ni_{0.48}Cu_{0.12}Zn_{0.4}Fe_2O_4$ (NCZ) by microwave hydrothermal method. Infrared Fourier Transform Spectroscopy (FTIR) was used to characterise the samples. Spinel and polymer phases were confirmed by the characterisation tests in the composite samples. Thermogravimetric analysis (TGA) and differential thermal analysis (DTA) were used to study the thermal properties of nanocomposites. It reveals that thermal stability is increased with ferrite content for the nanocomposites. The DC conductivity increased with polymer content.

1. Introduction

Polymer nanocomposites offer several notable benefits over conventional polymer composites, and they have the potential to be substantial. To attain the required characteristics of the composite material, the micron-sized composites typically need a high proportion of the filler phase. The nanocomposites, however, can attain the needed and superior qualities with a lot less filler. Low-density and high-processability materials will result from this [1,2]. Since they can display innovative magnetic, optical, thermal, electrical, and mechanical capabilities, nanoparticles have an advantage over micron-sized particles. Similar to this, the magnetic characteristics of nanoparticles, such as coercivity, saturation magnetization, and frequency-dependent permeability, differ significantly from those of micron-sized materials. The polymers offer a matrix that may be processed in which to spread the particles.

Polymer composites are widely used in a variety of industries, including the automotive sector [3–5] and the medical business as various types of sensors [6–8]. The suppression of electromagnetic interference (EMI) is a field in which polymer nanocomposites have various uses. Every electronic piece of equipment produces and emits radiofrequency waves, which can obstruct the functionality of both its own and other electronic components. Nowadays, as electronic gadgets become smaller, electromagnetic interference becomes a bigger issue since the electronic components must be packed closely together. A conductive surface reflects and absorbs energy from electromagnetic waves that have impacted it.

For modifying polymers for novel applications, knowledge of the thermal stability and degradation tendencies of polymer nanocomposites is helpful. The current work deals with the preparation of NCZ-PANI, and NCZ-PFD nanocomposites by mechanical alloying method. All the prepared samples were characterized and analysed using FTIR, TGA and DTA. DC conductivity properties were studied.

2. Experimental

2.1. Preparation of NiCuZnFe2O4

The high-grade (99.9%) chemicals nickel nitrate [Ni(NO3)2.6H2O], zinc nitrate [Zn(NO3)2.6H2O], copper nitrate [Cu(NO3)2.6H2O], and ferric nitrate [Fe(NO3)3.9H2O] from Sigma Aldrich were used to begin the process of making NCZ nanopowder. 50 cc of deionized water was used to dissolve these chemicals. To maintain a pH of 11.5, sodium hydroxide (NaOH) was added to the mixture. The precipitate was then moved into digesting containers and heated for 45 min at 160 °C for microwave hydrothermal treatment. The product is separated using the centrifugation technique, after which it is repeatedly cleaned with deionized water. The next step is drying in an oven for 10 h at 60 °C. The yield of the resulting powder, expressed as a percentage, is 96%. FTIR is then used to characterise the as-prepared Ni0.48Cu0.12Zn0.4Fe2O4 powder.

* Corresponding author.
E-mail address: panthagani.raju@gmail.com (P. Raju).

https://doi.org/10.1016/j.matpr.2023.06.303
2214-7853/© 20XX

2.2. Preparation of polyaniline

PANI was prepared by the polymerization process. At room temperature, aniline, hydrochloride and ammonium peroxydisulfate are mixed in an aqueous solution. The precipitate of PANI hydrochloride is then separated by filtering and dried. To prepare a 100 ml solution in a volumetric flask, equimolar proportions of aniline and hydrochloric acid are dissolved in distilled water. A 100 ml solution of APS is prepared by dissolving it in water at 0.25 M. In a beaker, both solutions are combined with a mechanical stirrer before being left to polymerize. After 24 h, the PANI precipitate is collected on a filter and washed with 300 cc of 0.2 M HCl and then with acetone. Polyaniline (emeraldine) powder is then dried in both air and vacuum at 60 °C.

Paraformaldehyde in solid form was purchased from Sigma Aldrich chemicals limited with 99% purity. The prepared polyaniline (PANI) and paraformaldehyde (PFD) powder were characterized by FTIR.

2.3. Preparation of NCZ-Polymer nanocomposites

The mechanical alloying process is used to prepare the nanocomposites of NCZ nanopowder, PANI, and PFD in various ratios. NCZ ferrite nanopowder and polymer powders are independently dried at 80 °C in an oven as they are fabricated and then cooled to room temperature. The powders are combined in varied ratios, (x) wt% NCZ + (1-x) wt% Polymer. Powders of each combination are processed individually in a RetschCo high-energy planetary ball mill for 15 h, pausing every 40 min for 5 min. The mill speed and ball-to-powder mass charge ratio are tuned and set at 300 rpm and 10:1, respectively. The blended powders are annealed for 30 min in an atmosphere of air at a temperature of 110 °C. Fourier infrared spectroscopy is used to characterise each nanocomposite sample (FTIR). The following composite sample was prepared, (x) wt% $Ni_{0.48}Cu_{0.12}Zn_{0.4}Fe_2O_4$ + (1-x) wt% Polyaniline, (x = 1, 0.9, 0.8, 0.7, 0.6, 0.5, 0) and labelled as NCZ, NP1, NP2, NP3, NP4, NP5, PANI, respectively, (x) wt% $Ni_{0.48}Cu_{0.12}Zn_{0.4}Fe_2O_4$ + (1-x) wt% Paraformaldehyde, (x = 1, 0.9, 0.7, 0.5, 0.3, 0.1, 0) and labelled as NCZ, NF1, NF2, NF3, NF4, NF5, PFD, respectively.

3. Results and discussions

Using Fourier Transform Infrared (FTIR) spectroscopy, the chemical compositions of nanocomposites were identified. Fig. 1 displays the FTIR spectra of nanocomposites made of different polyaniline fractions and ferrite (NCZ). Spinel ferrites (MFe_2O_4) have vibrational spectra that are ascribed to the inherent vibration of the tetrahedral sites in the high-frequency band (600–550 cm^{-1}), and the octahedral sites in the low-frequency band (440–400 cm^{-1}) [9,10]. The surfactant's C—O, C—O—C, and C—H groups are vibrating, which causes the bands at 1635 cm^{-1}, 1400 cm^{-1}, and 1122 cm^{-1} to be seen in ferrite. [11,12].

The typical polyaniline peaks are seen at 1612, 1558, 1473, 1145, 837, 617, and 503 cm^{-1}. The C—N vibration of the quinoid ring is responsible for the band that was seen at 1612 cm^{-1}. The bands in the spectra of PANI that absorb at 1558 cm^{-1} and 1473 cm^{-1}, respectively, are ascribed to the C—C stretching vibrations of the quinoid ring and the benzenoid ring, respectively. The stretching of the second aromatic amines' C-N bonds is shown by the band that first showed at 1145 cm^{-1}. At 837 cm^{-1}, the C—N+ polaron structure was seen to be extending. The protonated amine group on the backbone chain of the polyaniline is responsible for the absorption at 917 cm^{-1}. The aromatic ring deformation and the C—H bond's out-of-plane vibrations are represented by the band seen in the spectrum at 503 cm^{-1} [13].

The distinctive peaks of both ferrite and polyaniline emerged in the polyaniline-ferrite nanocomposite samples, as shown in Fig. 1. With a rise in PANI concentration, the NCZferrite characteristic peak that appears at 561 cm^{-1} shifts. With a drop in the weight % of ferrite in the nanocomposite, the peak at 561 cm^{-1}'s intensity reduced. The composites' bands that developed between 1400 and 1600 and at 1130 cm^{-1} demonstrate the coupling action of ferrite and polyaniline. All of the bands in these nanocomposites represent vibration modes in the ferrite matrix and are only slightly displaced from the FTIR spectra of pure PANI. This may suggest that the PANI and ferrite nanocrystals are generated simultaneously. Some FTIR bands of the PANI in the nanocomposites change as a result of polymer inclusion in the NCZ matrix. The findings indicate that PANI chains and NCZ ferrite interact, and they point to the potential for the production of NCZ-PANI nanocomposites.

Fig. 2 displays the FTIR spectra of the NCZ-PFD nanocomposites. The figure shows that the peaks at 3430 cm^{-1} and 2960 cm^{-1} are attributed to the C—H stretching vibration and the stretching of hydroxyl, respectively. The C—O—C symmetrical stretching vibration is linked to the peaks at 1250 cm^{-1} and 1110 cm^{-1}, whereas the peaks at 949 cm^{-1} and 841 cm^{-1} are related to the C—H bending wagging vibration and the deformation vibration of O—C—O of PFD, respectively [14,15]. In addition, the natural vibration of the tetrahedral and octahedral sites in the NCZ ferrite particles is what causes the absorption peaks at 576 cm^{-1} and 416 cm^{-1}. The vibration spectra of spinel ferrite show the presence of a high-frequency band (600–580 cm^{-1}) and a low-frequency band (440–400 cm^{-2}). The internal vibration of the tetrahedral and octahedral sites, respectively, is said to be the cause of

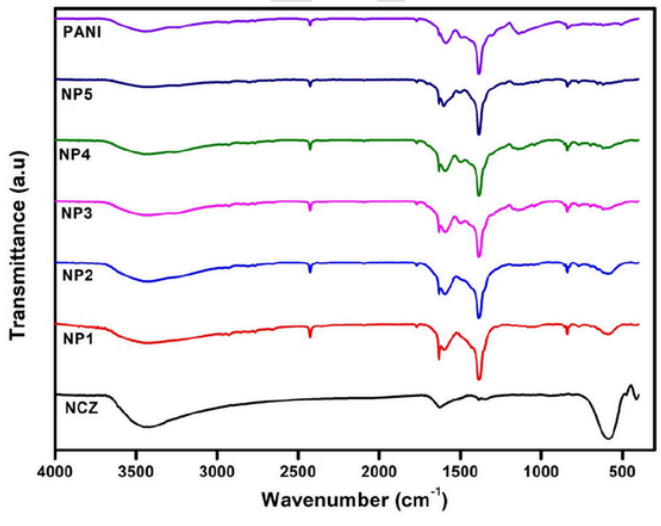

Fig. 1. FTIR spectra for NCZ-PANI nanocomposites.

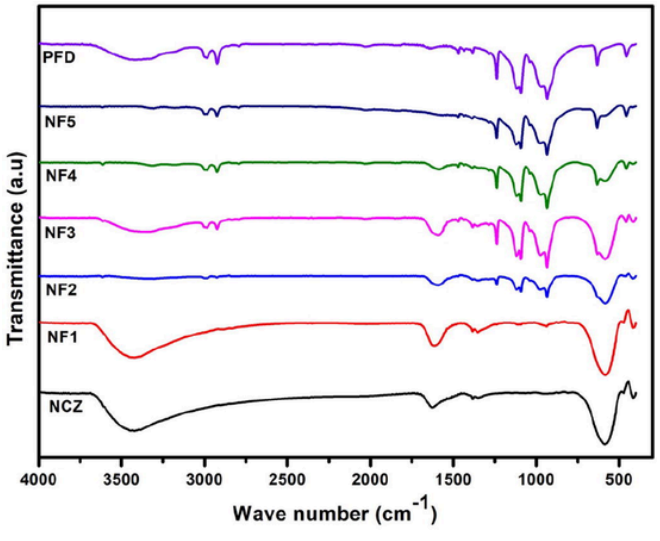

Fig. 2. FTIR spectra for NCZ-PFD nanocomposites samples.

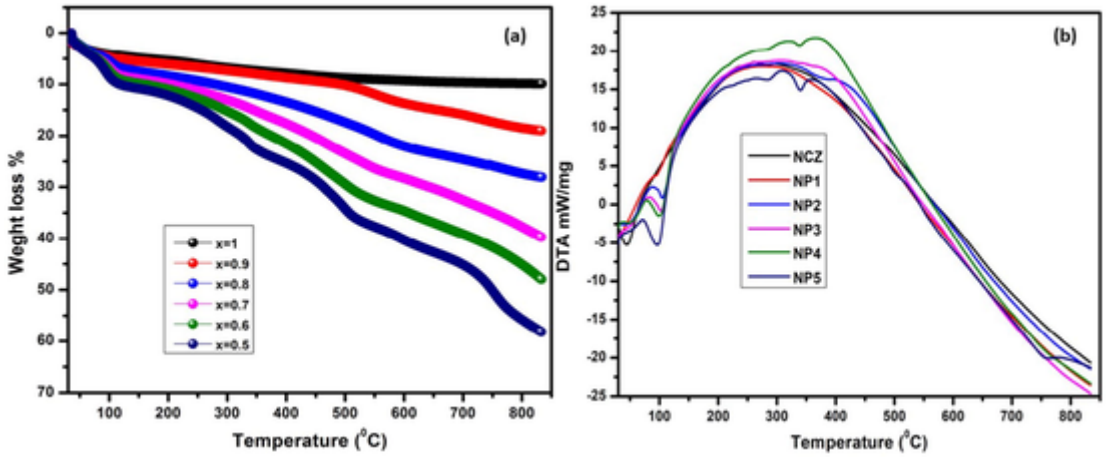

Fig. 3. A) tga and b) dta graphs for ncz-pani nanocomposites.

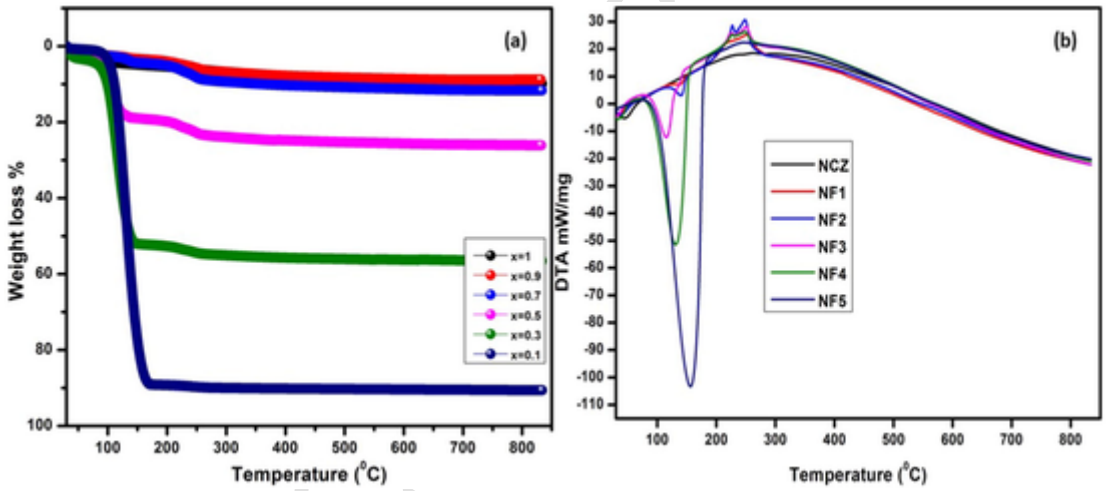

Fig. 4. A) tga and b) dta graphs for ncz-pfd nanocomposites.

these bands. These findings suggest that the PFD was evenly distributed across the ferrite matrix.

TGA and DTA studies were used to examine the thermal characteristics of nanocomposites and the interactions between ferrite and polyaniline. The TGA and DTA curves of NCZ and NCZ-PANI nanocomposites are shown in Fig. 3(a & b). The materials were heated in an inert environment of nitrogen gas from 30 to 850 °C at a constant rate of 10 °C/min. Different PANI to ferrite ratios in nanocomposites demonstrated various thermal deterioration stages. The weight loss was just around 8%, and the NiCuZn ferrite had remarkable thermal stability up to 850 °C. A minor endothermic peak in the DTA corresponds with the nanocomposites' TGA curve, which showed that the initial weight loss at 110 °C may be attributable to the loss of water and other volatile species (Fig. 3b). Gomes and Oliveira [16] corroborate this attribution. The elimination of water and dopant molecules adsorbed on polyaniline as well as the breakdown of oligomers are blamed for the weight loss below 250 °C.[17] The breakdown of the polyaniline's molecular chains is thought to be the third step in the degradation process.[11] Small aromatic fragments, substituted aromatic fragments, and extended aromatic fragments are created during the breakdown of polyaniline backbone chains.[16] As predicted, greater ferrite levels made the nanocomposites more resistant to heat deterioration. These thermograms show that the polyaniline in the nanocomposites has higher thermal stability, which may have been made possible by the potent surface contacts between the ferrite and polyaniline.

The TGA and DTA analyses of NICuZn ferrite and the NCZ-PFD nanocomposites in a nitrogen environment at a heating rate of 10 °C min^{-1} are shown in Fig. 4(a & b). The weight loss of the ferrite nanoparticles was slightly less than 8% since they were thermally stable. Three stages of heat deterioration were seen in nanocomposites with different PFD to ferrite ratios. We believe that the evaporation of free water molecules from the nanocomposite is what causes the weight loss up to 100 °C. As paraformaldehyde has a melting point of 120 °C, the highest weight loss below 150 °C is attributed to its evaporation. This is further supported by the deep endothermic peak in DTA plots (Fig. 4b). It has been shown that the maximum weight loss temperature in nanocomposites has somewhat increased; this might be the result of interaction between the ferrite and polymer particles.

A graph of the dc conductivity against PANI weight percentage for NCZ-PANI nanocomposites at room temperature is shown in Fig. 5. The graphic shows that the conductivity reduces as the amount of NCZ increases. The conductivity of NCZ-PANI nanocomposites may decrease with an increase in NCZ concentration because interactions between the polymer and NCZ nanoparticles may enhance charge carrier scattering and, as a result, increase the sample's resistivity [18,19]. Increased charge carrier trapping caused by the nanoparticles themselves, as well as imperfections and morphological changes they create, might have additional impacts. We proposed the creation of polarons upon oxidation of the polyaniline molecule and the combining of two nearby polarons to create a bipolaron as a possible explanation for the conductive behaviour in our samples. The outcome is the development of a bipo-

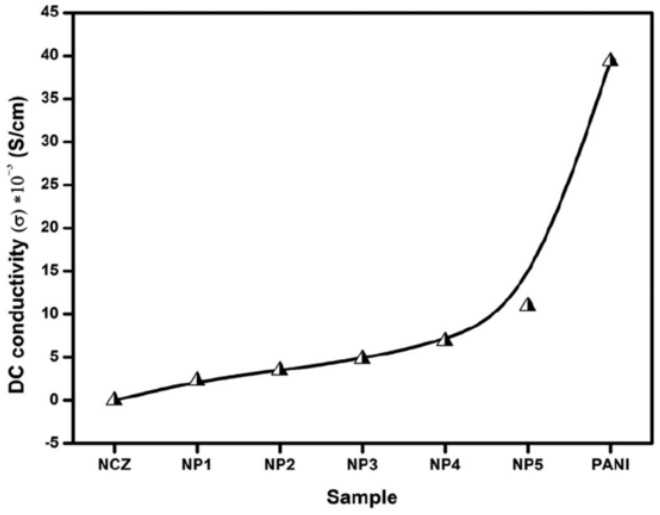

Fig. 5. DC conductivity of NCZ-PANI nanocomposites at room temperature.

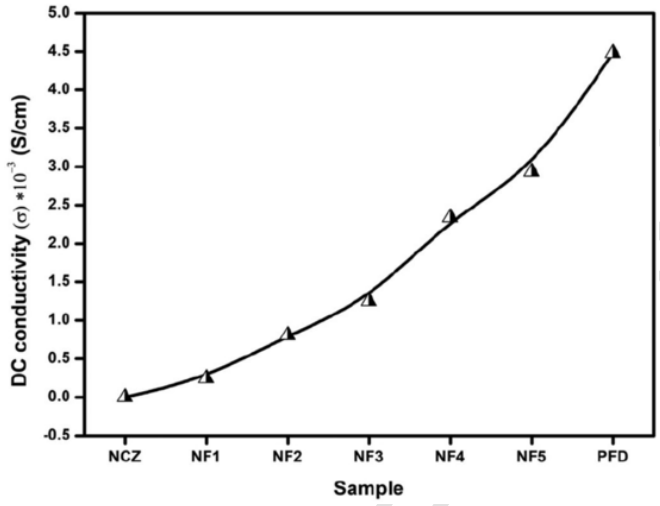

Fig. 6. DC conductivity of NCZ-PFD nanocomposites at room temperature.

laron, a defect that is doubly charged and delocalized throughout many polyaniline rings.

The conductivity of the NCZ, PFD, and NCZ-PFD nanocomposites at room temperature is shown in Fig. 6. The conductivity of the resultant nanocomposites is considerably impacted by the addition of PFD polymer. The insulating behaviour of the iron oxide in the core of the nanoparticles, which prevents charge transfer and lowers conductivity, is responsible for the reduction in conductivity of nanocomposites with increasing ferrite concentration. When the polymer forms chains, the electrical resistivity of the composites is greatly lowered due to the low resistivity of the polymer phase, which may also explain why conductivity increases with an increase in PFD concentration.

4. Conclusions

NCZ-PANI and NCZ-PFD nanocomposites were successfully prepared using the mechanical milling method. The FTIR spectra of nanocomposites show all characteristic peaks corresponding to NCZ, PANI, and PFD respectively. No impurity phases were observed. The incorporation of polymer with NCZ ferrite leads to shifting some FTIR bands of the polymer in the nanocomposites. The results reveal that there exists an interaction between ferrite and polymer chains, and suggests the effective formation of the NCZ-polymer nanocomposites. From the studies of thermal analysis, it was found that the NCZ-PANI nanocomposites show good temperature stability and it is increased with ferrite content. There is no considerable change is observed for the NCZ-PFD nanocomposites. The d.c conductivity (σ_{dc}) measurements were carried out on all the samples of NCZ-PANI and NCZ-PFD nanocomposites by using the two-probe method conductivity increases with polymer content.

Declaration of Competing Interest

The authors declare that they have no known competing financial interests or personal relationships that could have appeared to influence the work reported in this paper.

Data availability

Data will be made available on request.

References

[1] M.A. Kashfipour, N. Mehra, J. Zhu, A review on the role of interface in mechanical, thermal, and electrical properties of polymer composites, Adv. Compos. Hybrid Mater. 1 (2018) 415–439.
[2] J. Jordan, K.I. Jacob, R. Tannenbaum, M.A. Sharaf, I. Jasiuk, Experimental trends in polymer nanocomposites—a review, Mater. Sci. Eng., A. 393 (1–2) (2005) 1–1.
[3] K. Palani Kumar, D. Keshavan, E. Natarajan, A. Narayan, K. Ashok Kumar, M. Deepak, L.I. Freitas, Evaluation of mechanical properties of coconut flower cover fibre-reinforced polymer composites for industrial applications, Prog. Rubber Plast. Recycl. Technol. 37 (1) (2021) 3–18.
[4] S. Kharbanda, T. Bhadury, G. Gupta, D. Fuloria, P.R. Pati, V.K. Mishra, A. Sharma, Polymer composites for thermal applications–A review, Mater. Today Proc. 47 (2021) 2839–2845.
[5] I.O. Oladele, T.F. Omotosho, A.A. Adediran, Polymer-based composites: An indispensable material for present and future applications, J. Polym Sci. 2020 (2020) 1–2.
[6] S. Cichosz, A. Masek, M. Zaborski, Polymer-based sensors: A review, Polym. Test. 67 (2018) 342–348.
[7] R. Dersch, M. Steinhart, U. Boudriot, A. Greiner, J.H. Wendorff, Nanoprocessing of polymers: applications in medicine, sensors, catalysis, photonics, Polym. Adv. Technol. 16 (2–3) (2005) 276–282.
[8] Y. Saylan, S. Akgönüllü, H. Yavuz, S. Ünal, A. Denizli, Molecularly imprinted polymer based sensors for medical applications, Sensors 19 (6) (2019) 1279.
[9] P. Priyadharsini, A. Pradeep, P.S. Rao, G. Chandrasekaran, Structural, spectroscopic and magnetic study of nanocrystalline Ni–Zn ferrites, Mater. Chem. Phys. 116 (1) (2009) 207–213.
[10] M.R. Patil, M.K. Rendale, S.N. Mathad, R.B. Pujar, FTIR spectra and elastic properties of Cd-substituted Ni–Zn ferrites, Int. J. Self Propag. High Temp. Synth. 26 (2017) 33–39.
[11] W. Wang, S.P. Gumfekar, Q. Jiao, B. Zhao, Ferrite-grafted polyaniline nanofibers as electromagnetic shielding materials, J. Mater. Chem. C. 1 (16) (2013) 2851–2859.
[12] A. Rushiti, T. Falk, M. Muhler, C. Hättig, Interactions of water and short-chain alcohols with CoFe 2 O 4 (001) surfaces at low coverages, Phys. Chem. Chem. Phys. 24 (38) (2022) 23195–23208.
[13] S. Xuan, Y.X. Wang, J.C. Yu, K.C. Leung, Preparation, characterization, and catalytic activity of core/shell Fe3O4@ polyaniline@ Au nanocomposites, Langmuir 25 (19) (2009) 11835–11843.
[14] A.S. Giroto, S.F. do Valle, G.G. Guimarães, N.D. Jablonowski, C. Ribeiro, L.H. Mattoso, Different Zn loading in Urea-Formaldehyde influences the N controlled release by structure modification, Sci. Rep. 11 (1) (2021) 1–2.
[15] Y.S. Park, Y. Ito, Y. Imanishi, pH-controlled gating of a porous glass filter by surface grafting of polyelectrolyte brushes, Chem. Mater. 9 (12) (1997) 2755–2758.
[16] E.C. Gomes, M.A. Oliveira, Chemical polymerization of aniline in hydrochloric acid (HCl) and formic acid (HCOOH) media. Differences between the two synthesized polyanilines, Am. J. Polym. Sci. 2 (2) (2012) 5–13.
[17] A.H. Elsayed, M.M. Eldin, A.M. Elsyed, A.A. Elazm, E.M. Younes, H.A. Motaweh, Synthesis and properties of polyaniline/ferrites nanocomposites, Int. J. Electrochem. Sci. 6 (1) (2011) 206–221.
[18] M. Khairy, M.E. Gouda, Electrical and optical properties of nickel ferrite/polyaniline nanocomposite, J. Adv. Res. 6 (4) (2015) 555–562.
[19] N.N. Ali, Y. Atassi, A. Salloum, A. Charba, A. Malki, M. Jafarian, Comparative study of microwave absorption characteristics of (Polyaniline/NiZn ferrite) nanocomposites with different ferrite percentages, Mater. Chem. Phys. 211 (2018) 79–87.